

STRESS CONCENTRATION AT LOAD-CARRYING FILLET WELDED CRUCIFORM JOINTS SUBJECTED TO TENSILE AND BENDING LOADS

Krzysztof L. MOLSKI*

*Bialystok University of Technology, ul. Wiejska 45C, 15-351 Bialystok, Poland

k.molski@pb.edu.pl

received 25 November 2019, revised 13 December 2019, accepted 18 December 2019

Abstract: This article presents numerical finite element method (FEM) analysis of the stress concentration at toes and crack-like faults in load-carrying fillet welded cruciform joints with transversal slits resulting from non-fused root faces. Potential fatigue damage of such joints subjected to cyclic tensile and bending loads appears in the form of fatigue cracks starting from the weld roots or toes. The aim of this article is to find qualitative and quantitative relationships between geometrical parameters of the load-carrying fillet welded cruciform joint subjected to tensile and bending loads and the stress concentration at weld toes and roots. The results of the analysis represented by the stress concentration factors (SCFs) and the stress intensity factors K_I and K_{II} are shown in the form of tables, graphs and mathematical formulas, which may be applied for fatigue assessment of such joints.

Key words: cruciform welded joint, load-carrying fillets, stress concentration factor, stress intensity factor, finite element method

1. INTRODUCTION

Cruciform welded joints are commonly used in engineering practice. There are two general types of such connections known as the 'non-load carrying fillet welded joints' and the 'load-carrying fillet welded joints'. In the first type, the external loads are sustained by the main plate with additional transversal stiffeners, whereas, in the latter, the loads pass through the fillet welds. Besides, both types of joints may have un-fused root faces producing the so-called 'lack of penetration defects'.

It is well known that fatigue fracture produced by fluctuating loads is the most common damage mechanism of welded connections. Therefore, the weakest points determining fatigue life of the structure are related to particular zones of high stress concentration located at a weld toe and at the apex of existing slits. Fatigue life of such connections may be estimated in many ways, taking into account possible damage mechanisms, including crack location and its possible growth. Some details of different approaches used for the assessment of fatigue life can be found in the literature (e.g. in Peterson, 1974; Monahan, 1995; Singh et al., 2002; Chung et al., 2008; Wooryong and Chitoshi, 2008; Radaj et al., 2009; Chattopadhyay et al., 2011; Sonsino et al., 2012; Singh et al., 2003; Livieri and Lazzarin, 2005; Dong, 2001; Lotsberg and Sigurdsson, 2006; Stenberg et al., 2015; Remes, and Varsta, 2010; Kranz and Sonsino, 2010; Schijve, 2012; Zerbst et al., 2016; Niemi et al., 2018; Tchoffo et al., 2017). Numerous design procedures have also been developed and published in the form of standards and recommendations (e.g. Young and Lawrence, 1985; CES, 2005; Hobbacher, 2009; Fricke, 2012; Fricke, 2013; ISO, 2013). Many solutions to stress concentration factors (SCFs) regarding various types of weldments have also been published (e.g. in Ushirokawa and Nakayama, 1983; Tsuji, 1990; Iida and Uemura, 1996; Molski et al., 2019).

The assessment of fatigue life requires high accuracy of SCFs solutions. As shown in Molski et al. (2019), several percentages of errors in estimating maximum stress range may lead in some circumstances up to 200% inaccuracy in estimating fatigue life. Therefore, SCF approximation formulas should be highly accurate and cover wide range of values of all basic geometrical parameters, determining shape of the joint and influencing SCF.

The fatigue strength of the load-carrying fillet welded cruciform joints with the lack of penetration defects is generally lower than that for the non-load carrying joints because of the fact that un-fused root faces are in transverse position to the main plate. Such a location of both slits may produce high stress concentration at the vicinity of each apex and additionally increases the maximum stress at the weld toe.

The present work deals with the determination of SCFs and the stress intensity factors K_I and K_{II} in the weld region of a load-carrying fillet welded cruciform joint subjected to tensile and bending loads.

2. GENERAL ASSUMPTIONS AND MODELLING STRATEGY

The shape and the basic geometrical parameters of the joint under consideration subjected to tensile and bending loads are shown in Figure 1. Two zones located at the weld toe and at the apex of the slit, denoted by A and B, respectively, represent the places where significant increase of stresses is expected.

As the toe radius $\rho > 0$, the maximum stress is finite and can be represented by the stress concentration factor K_t^t for tensile and K_b^t for bending load, respectively. In the case of un-fused crack-like defect, two stress intensity factors have to be determined separately for each loading mode. For convenience, both SCFs for tension and bending may be represented by the following equations:

$$K_t^t = K_{t0}^t F^t \tag{1}$$

$$K_t^b = K_{t0}^b F^b \tag{2}$$

as a product of the known stress concentration factors K_{t0}^t and K_{t0}^b for fully penetrated welds and the unknown correction functions F^t and F^b that have to be determined. An extended review of published formulas dealing with K_{t0}^t and K_{t0}^b for these weldments is presented in Ushirokawa and Nakayama (1983) Tsuji (1990) and Iida and Uemura (1996), and, therefore, they will not be quoted here.

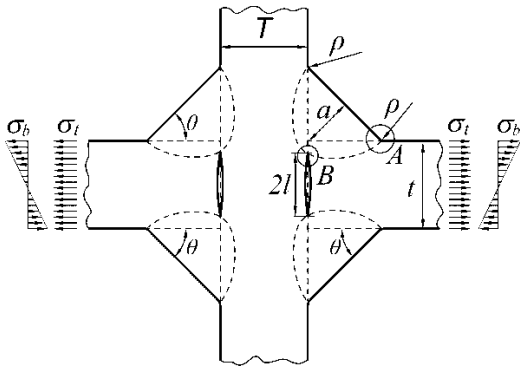


Fig. 1. General shape and loading conditions of the load-carrying fillet welded cruciform joint with two crack-like slits

In the case of stress intensity factors K_I and K_{II} , it is convenient to introduce the following general formula:

$$K_j = \sigma \sqrt{\pi l} F_{K_j} \tag{3}$$

where σ represents the remote nominal stress and F_{K_j} is a correction function that has to be determined. The subscript j indicates the loading mode of the joint.

There are several geometrical parameters characterising the shape of the weldment, as weld toe radius ρ , nominal throat thickness a , weld face angle θ , thickness of the main plate t and so on. It was supposed that the weld face angle $\theta = 45^\circ$ and the ratios of other parameters change in the following ranges: $0.1 \leq \rho/a \leq 0.5$, $0.25 \leq a/t \leq 1$, $0 \leq 2l/t \leq 1$ and $0.5 \leq T/t \leq 2$, which usually apply to weldments in engineering structures. Many particular values of geometrical parameters were chosen in each range depending on the values of calculated correction functions. For example, the ρ/a parameter was changed by a step of 0.1, whereas T/t parameter was changed by a step of 0.5. In cases of two remaining parameters, 5 – 10 different values were chosen from the appropriate range.

Numerical finite element method (FEM) modelling of the joint has been carried out using ANSYS 19 MultiPhysics program and PLANE 182 type of finite elements. The material of the body is linear-elastic, isotropic and homogeneous. Small deformations occur because of external load. Both load-carrying main plates of the same thickness t are co-linear, and the shape of all fillet welds is identical.

Shape of the body as well as loading and displacement boundary conditions of the cruciform joints are shown in Figure 2.

About 200,000 finite elements were used for each model and a special attention has been given to the finite element mesh density at the weld critical zones A and B, which is shown in Figure 3. In the first case, the arc of the toe radius ρ was described by at least 40 elements. In the second case, the use of a very fine mesh was necessary with special triangular elements located at the core around the crack tip. Such a modelling strategy is appropriate for approximating the stress singularity and makes the stress field around the crack tip proportional to $r^{-0.5}$ according to the exact analytical solution based on the theory of elasticity.

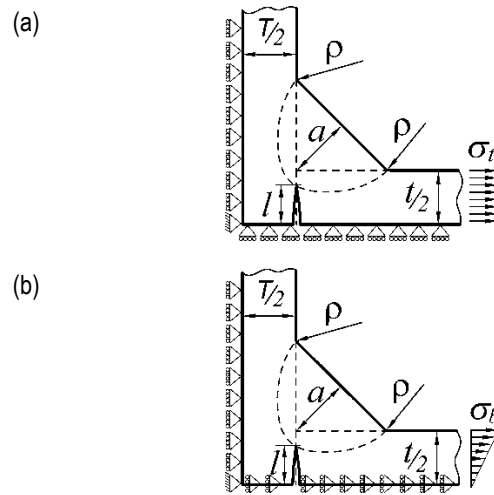


Fig. 2. Geometry and loading conditions – (a) tensile and (b) bending – of the modelled element

3. RESULTS AND DISCUSSION

Several hundred numerical FEM solutions have been obtained for the loaded joints, which are shown in Figure 2. One example of such a solution for tensile load is presented in Figure 3, where critical zones of increased stress concentration are clearly seen.

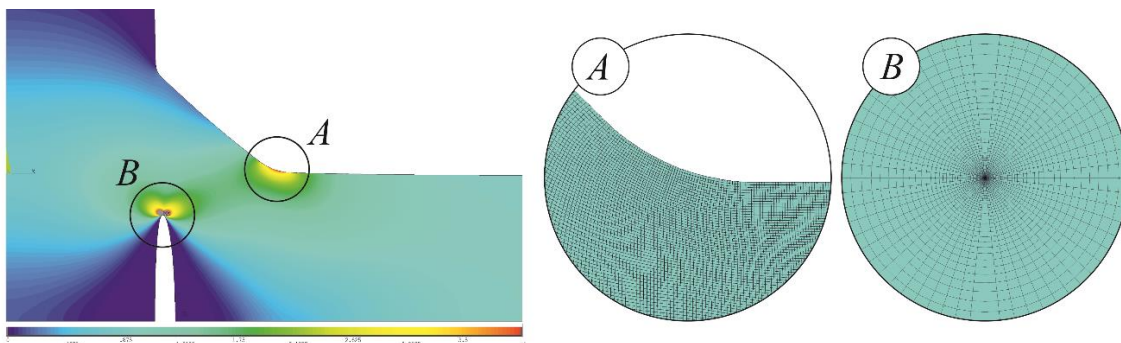


Fig. 3. Distribution of the principal stress component σ_1 in the joint subjected to tension. Details A and B show the finite element mesh in both critical zones

The calculated maximum principal stresses at the weld toe were compared to the nominal ones and divided by the particular reference values of K_{t0}^t and K_{t0}^b obtained in the same way for joints without the lack of penetration defects. Such a procedure made it possible to calculate particular values of correction parameters F^t and F^b using equations (1) and (2). Using equation (3), the values of correction parameters $F_{K_j}^t$ and $F_{K_j}^b$ have been obtained in a similar way.

The detailed analysis of the results led to the conclusion that two shape parameter ratios l/t and a/t are the most important and have significant impact on the values of all correction parameters. Other geometrical ratios of p/a and T/t have minor influence on all F^t , F^b , $F_{K_j}^t$ and $F_{K_j}^b$. The maximum changes in correction parameters for the weld toe because of p/a and T/t are about 5%, whereas for the apex of the transverse, cracks do not exceed 1%. It is also important to note that for tensile loading, the stress intensity factor, K_{II} , is about 8–15 times lower than K_I and, therefore, may be omitted in the procedures of fatigue life assessment.

In the case of bending load, both stress intensity factors K_I and K_{II} are of the same order. In spite of the fact that their values are much lower than K_I for tension under the same nominal stress, both loading modes – tension and bending – are independently applied in the real structures, which means that their proportions are generally not known.

It is important to note that from a theoretical point of view, if pure bending load is applied, one half of the central slit is open, whereas the other tends to be closed. As mutual penetration of both crack faces under compression is not physically possible, some additional comments are necessary. Generally, there are two reasons confirming the solution is reasonable. The first reason is that welding process never introduces a perfect crack. The un-fused faces are usually slightly separated and such a penetration may not occur or may be very limited. The second reason is that bending load usually acts together with the accompanying tensile load, producing additional opening of the slit. This leads to the conclusion that real conditions inside the weldment are in fact unknown and the assumptions made here are rational enough to explain the applicability of the solution to the assessment of fatigue life.

Some examples of particular values of correction parameters, transformed later into correction functions are presented in Tables 1–5 and shown in Figures 4–8. Mathematical formulas (A1)–(A5) derived from numerical solutions and appropriate for the assessment of fatigue life of the load-carrying fillet welded cruciform joint are presented in Appendix. The accuracy of those equations does not exceed 1% compared to the numerical FEM solutions.

Table 1. Numerical values of the correction function F^t

$p/a=0.5$		$2l/t$					
a/t	K_{t0}^t	0.0	0.25	0.50	0.75	0.90	1.0
0.25	2.207	1.0	1.072	1.311	1.773	2.179	2.502
0.333	2.053	1.0	1.061	1.245	1.558	1.809	2.002
0.4	1.960	1.0	1.048	1.190	1.420	1.599	1.734
0.6	1.759	1.0	1.020	1.077	1.167	1.237	1.289
0.8	1.624	1.0	1.007	1.028	1.061	1.087	1.107
1.0	1.526	1.0	1.003	1.009	1.021	1.029	1.035

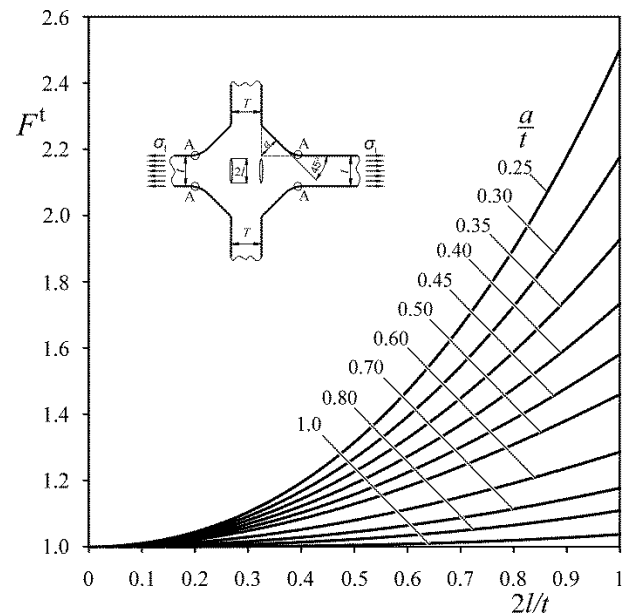


Fig. 4. Correction function F^t for calculating $K_{K_j}^t$ at a weld toe of a load-carrying fillet welded cruciform joint with a lack of penetration defect and subjected to tensile load

Table 2. Numerical values of correction function $F_{K_j}^t$

a/t	$2l/t$					
	0.10	0.25	0.50	0.75	0.90	1.0
0.25	0.826	0.832	0.868	0.960	1.051	1.131
0.333	0.786	0.788	0.807	0.859	0.910	0.954
0.4	0.752	0.751	0.759	0.791	0.824	0.823
0.6	0.648	0.643	0.635	0.638	0.646	0.655
0.8	0.562	0.554	0.541	0.534	0.534	0.537
1.0	0.492	0.485	0.471	0.459	0.456	0.456

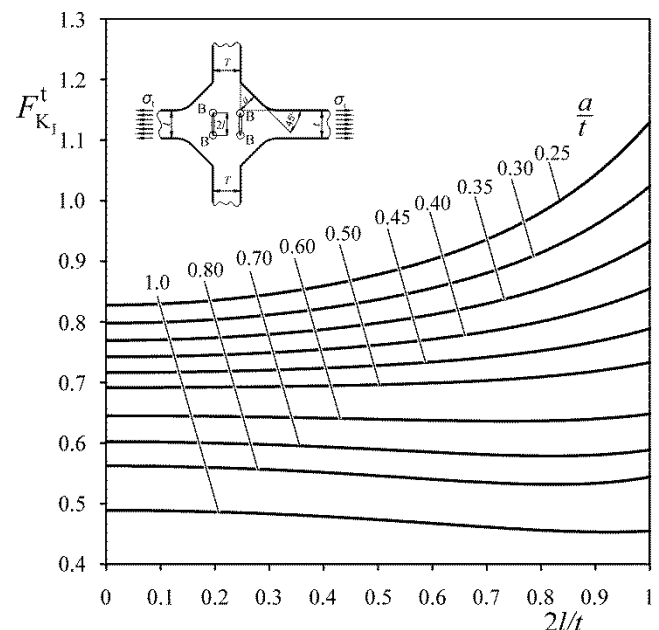


Fig. 5. Correction function $F_{K_j}^t$ for calculating $K_{K_j}^t$ at the apex of a lack of penetration defect in the load-carrying fillet welded cruciform joint subjected to tensile load

Table 3. Numerical values of the correction function F^b

$\rho a=0.5$		$2l/t$					
alt	K_{t0}^b	0.0	0.25	0.50	0.75	0.90	1.0
0.25	1.784	1.0	1.011	1.052	1.143	1.223	1.282
0.333	1.647	1.0	1.006	1.027	1.065	1.095	1.115
0.4	1.568	1.0	1.003	1.014	1.033	1.046	1.056
0.6	1.416	1.0	1.0	1.001	1.003	1.005	1.006
0.8	1.328	1.0	1.0	1.0	1.0	1.0	1.0
1.0	1.271	1.0	1.0	1.0	1.0	1.0	1.0

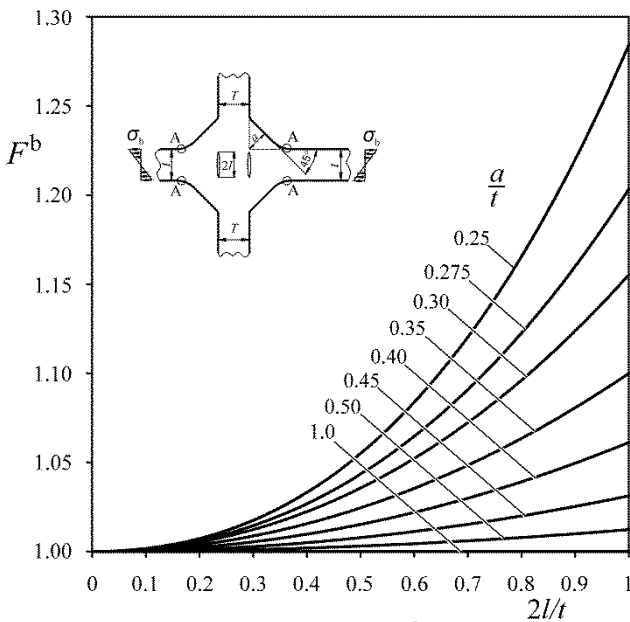


Fig. 6. Correction function F^b for calculating K_t^b at a weld toe of a load-carrying fillet welded cruciform joint with a lack of penetration defect and subjected to bending load

Table 4. Numerical values of the correction function $F_{K_I}^b$

alt	$2l/t$					
	0.10	0.25	0.50	0.75	0.90	1.0
0.25	0.026	0.066	0.133	0.198	0.238	0.264
0.333	0.022	0.054	0.106	0.153	0.177	0.193
0.4	0.018	0.045	0.088	0.125	0.144	0.155
0.6	0.011	0.026	0.051	0.072	0.083	0.089
0.8	0.006	0.016	0.031	0.045	0.052	0.056
1.0	0.004	0.010	0.021	0.030	0.034	0.037

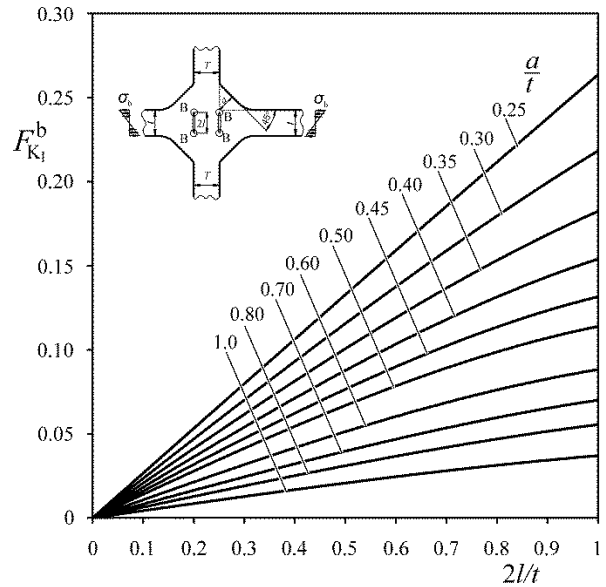


Fig. 7. Correction function $F_{K_I}^b$ for calculating $K_{K_I}^b$ at the apex of a lack of penetration defect in the load-carrying fillet welded cruciform joint subjected to bending load

Table 5. Numerical values of the correction function $F_{K_{II}}^b$

alt	$2l/t$					
	0.10	0.25	0.50	0.75	0.90	1.0
0.25	0.127	0.126	0.117	0.102	0.090	0.080
0.333	0.114	0.111	0.101	0.086	0.075	0.068
0.4	0.100	0.098	0.088	0.075	0.066	0.060
0.6	0.066	0.064	0.059	0.051	0.046	0.042
0.8	0.043	0.043	0.040	0.035	0.033	0.031
1.0	0.029	0.029	0.028	0.025	0.024	0.023

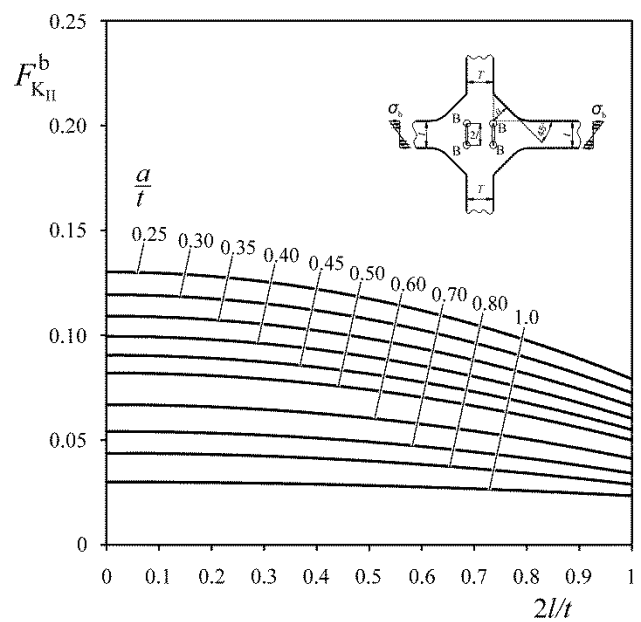


Fig. 8. Correction function $F_{K_{II}}^b$ for calculating $K_{K_{II}}^b$ at the apex of a lack of penetration defect in the load-carrying fillet welded cruciform joint subjected to bending load

The correction formula (4) proposed by Ushirokawa and Nakayama (1983), reported also in Iida and Uemura (1996), and represented in parameters regarded in the present work, also deals with the increase in SCF at the weld toe of a load-carrying fillet joint subjected to tensile load and should correspond to the present solution given by equation (A1).

$$F_{UN}^t = 1 + 0.64 \frac{(2l/t)^2}{2\sqrt{2}a/t} - 0.12 \frac{(2l/t)^4}{(2\sqrt{2}a/t)^2} \quad (4)$$

Comparison of both equations have shown significant differences in calculating correction values up to 33% in the range of $0.25 \leq a/t \leq 0.5$ and about $\pm 5\%$ in the range of $0.5 \leq a/t \leq 1$.

4. CONCLUSIONS

An extended analysis of numerical FEM solutions carried out using the ANSYS 19 MultiPhysics program for the load-carrying fillet welded cruciform joint with the lack of penetration defects has shown the significant influence of the geometrical parameters a , l and t of the weldment on the stress concentrations at two critical zones: at the weld toe and at the weld root. The first effect is represented by the correction functions of the stress concentration factor, whereas the second may be quantitatively described by the stress intensity factors K_I and K_{II} commonly used in fracture mechanics. The influence of the other parameters ρ and T has a minor effect.

Five correction functions have been derived, making it possible to calculate the corrected values of the stress concentration factors at the weld toe and particular values of K_I and K_{II} at the weld root for tensile and bending loads. For tensile load, K_{II} is 8–15 times smaller than K_I and may be omitted in the assessment of fatigue life. The accuracy of the formulas compared to the FEM results does not exceed 1.5%. The formulas presented in Appendix facilitate the computer-aided assessment of fatigue life of the structural element with such welded connections.

The correction formula of Ushirokawa and Nakayama (4) differs from the present solution given by equations (A1) of about $\pm 5\%$ in the range of $0.5 \leq a/t \leq 1$ and provides underestimated values up to -33% for the lower a/t ratios in the range of $0.25 \leq a/t \leq 0.5$.

Appendix: Formulas for calculating SCFs and stress intensity factors at the critical zones of a load-carrying fillet welded cruciform joint containing lack of penetration defects

Range of application: $0 < \rho/a \leq 0.5$; $0.25 \leq a/t \leq 1$; $0 \leq 2l/t \leq 1$ and $0.5 \leq T/t \leq 2$.

Tensile load, SCF at a weld toe:

$$K_t^t = K_{t0}^t F^t \quad (A1)$$

where

$$F^t = 1 + A_1(2l/t)^2 + A_2(2l/t)^3$$

$$A_1 = \text{Exp}(-5.25(a/t)^3 + 0.103)$$

$$A_2 = 4.028 - 24.433(a/t) + 51.482(a/t)^2 - 45.700(a/t)^3 + 14.655(a/t)^4$$

Tensile load, mode I stress intensity factor:

$$K_I^t = \sigma_t \sqrt{\pi l} F_{K_I}^t \quad (A2)$$

where

$$F_{K_I}^t = 1 + B_1 + B_2(2l/t)^2 + B_3(2l/t)^6$$

$$B_1 = -0.774(a/t) + 0.366(a/t)^2 - 0.103(a/t)^3$$

$$B_2 = 0.489 - 1.434(a/t) + 1.086(a/t)^2 - 0.204(a/t)^3$$

$$B_3 = 0.439 - 2.013(a/t) + 3.126(a/t)^2 - 1.523(a/t)^3$$

Bending load, SCF at a weld toe:

$$K_t^b = K_{t0}^b F^b \quad (A3)$$

where

$$F^b = 1 + C_1(2l/t)^2 + C_2(2l/t)^3$$

$$C_1 = \text{Exp}(-43.228(a/t)^4 - 1.693)$$

$$C_2 = \text{Exp}(-58.566(a/t)^2 + 1.613)$$

Bending load, mode I stress intensity factor:

$$K_I^b = \sigma_b \sqrt{\pi l} F_{K_I}^b \quad (A4)$$

where

$$F_{K_I}^b = D_1(2l/t) + D_2(2l/t)^3$$

$$D_1 = 0.470 - 0.999(a/t) + 0.786(a/t)^2 - 0.214(a/t)^3$$

$$D_2 = 0.233 - 1.713(a/t) + 3.939(a/t)^2 - 3.737(a/t)^3 + 1.272(a/t)^4$$

Bending load, mode II stress intensity factor:

$$K_{II}^b = \sigma_b \sqrt{\pi l} F_{K_{II}}^b \quad (A5)$$

where

$$F_{K_{II}}^b = E_1 + E_2(2l/t)^2$$

$$E_1 = 0.193 - 0.281(a/t) + 0.118(a/t)^2$$

$$E_2 = -0.074 + 0.100(a/t) - 0.033(a/t)^2$$

List of symbols:

a , nominal weld throat thickness; F^t , correction function of K_{t0}^t for partial penetration welds; F^b , correction function of K_{t0}^b for partial penetration welds; $F_{K_I}^t$, correction function of K_I for tensile load; $F_{K_I}^b$, correction function of K_I for bending load; $F_{K_{II}}^b$, correction function of K_{II} for bending load; FEM, finite element method; $2l$, total length of a crack or slit appearing as a consequence of unfused root faces; K_I^t , mode I stress intensity factor for cracks or unfused slits, tensile load; K_{II}^t , mode II stress intensity factor for cracks or unfused slits, tensile load; K_I^b , mode I stress intensity factor for cracks or unfused slits, bending load; K_{II}^b , mode II stress intensity factor for cracks or unfused slits, bending load; $K_t^t = \sigma_{\text{max}}/\sigma_t$, weld toe stress concentration factor for partial pene-

tration welds (tension); $K_t^b = \sigma_{1\max}/\sigma_b$, weld toe stress concentration factor for partial penetration welds (bending); $K_{t0}^t = \sigma_{1\max}/\sigma_t$, weld toe stress concentration factor for full penetration welds (tension); $K_{t0}^b = \sigma_{1\max}/\sigma_b$, weld toe stress concentration factor for full penetration welds (bending); r , radial distance measured from the crack tip; SCF, stress concentration factor; t , thickness of the main plate; T , thickness of the transversal plate; ρ , weld toe radius; σ_t , nominal tensile stress; σ_b , nominal bending stress; $\sigma_{1\max}$, maximum principal stress at a weld toe.

REFERENCES

1. **Chattopadhyay A, Glinka G, El-Zein M, Qian J, Formas R.** (2011), Stress analysis and fatigue of welded structures, *Weld World*, 55(7–8), 2–21.
2. **Chung HY., Liu SH., Lin RS., Ju SH.** (2008), Assessment of stress intensity factors for load-carrying fillet welded cruciform joints using a digital camera, *Int. Journal of Fatigue*, 30(10–11), 1861–1872.
3. **Dong P.** (2001), A structural stress definition and numerical implementation for fatigue analysis of welded joints, *Int. Journal of Fatigue*, 23(10), 865–876.
4. **European Committee for Standardization (CES)** (2005), *Eurocode 3: Design of steel structures - Part 1–9, Fatigue*, Brussels: CES; EN 1993-1-9:2005.
5. **Fayard JL., Bignonnet A. and Dang Van K.** (1996), Fatigue design criteria for welded structures, *Fatigue Fracture Eng. Materials & Structures*, 19(6), 723–729.
6. **Fricke W.** (2012), IIW Recommendations for the Fatigue Assessment of Welded Structures by Notch Stress Analysis: IIW-2006-09, *Woodhead Publishing Series in Welding and Other Joining Technologies*, 2–41.
7. **Fricke, W.** (2013), IIW guideline for the assessment of weld root fatigue, *Weld World*, 57, 753.
8. **Hobbacher A.F.** (2009), The new IIW recommendations for fatigue assessment of welded joints and components – A comprehensive code recently updated, *International Journal of Fatigue*, 31, 50–58.
9. **Iida K., Uemura T.,** (1996), Stress concentration factor formulas widely used in Japan, *Fatigue Fract Eng Mater Struct.*, 19(6), 779–786.
10. **ISO 9692-1** (2013) *Welding and allied processes — Types of joint preparation — Part 1: Manual metal arc welding, gas-shielded metal arc welding, gas welding, TIG welding and beam welding of steels.*
11. **Kranz B., Sonsino C.M.** (2010), Verification of FAT Values for the Application of the Notch Stress Concept with the Reference Radii $R_{ref} = 1.00$ and 0.05 mm, *Weld World*, 54(7–8), 218–224.
12. **Livieri P., Lazzarin, P.** (2005), Fatigue strength of steel and aluminium welded joints based on generalised stress intensity factors and local strain energy values, *Int. Journal of Fracture*, 133(3), 247–276.
13. **Lotsberg I., Sigurdsson G.** (2006), Hot Spot Stress S-N Curve for Fatigue Analysis of Plated Structures, *J. Offshore Mech. Arct. Eng.*, 128(4), 330–336.
14. **Molski K.L., Tarasiuk P., Glinka G.** (2019), *Description of stress concentration at tee welded joints subjected to tensile and bending loads*, Opole University of Technology, Oficyna Wydawnicza, Studia i Monografie, 516, 61–80 (in Polish).
15. **Monahan C.C.** (1995), *Early fatigue cracks growth at welds*, Computational Mechanics Publications, Southampton.
16. **Niemi E., Fricke W. Maddox S. J.** (2018), *Structural Hot-Spot Stress Approach to Fatigue Analysis of Welded Components*, <https://doi.org/10.1007/978-981-10-5568-3>.
17. **Peterson R.E.** (1974), *Stress concentration design factors*, 2nd ed., Wiley, New York.
18. **Radaj D., Sonsino CM., Fricke W.** (2009), Recent developments in local concepts of fatigue assessment of welded joints, *International Journal of Fatigue*, 31(1), 2–11.
19. **Remes, H., Varsta, P.** (2010), Statistics of Weld Geometry for Laser-Hybrid Welded Joints and its Application within Notch Stress Approach, *Weld World*, 54(7–8), 189–207.
20. **Schijve J.** (2012), Fatigue predictions of welded joints and the effective notch stress concept, *International Journal of Fatigue*, 45, 31–38.
21. **Singh P.J., Achar D.R.G., Guha B., Nordberg H.** (2002), Influence of weld geometry and process on fatigue crack growth characteristics of AISI 304L cruciform joints containing lack of penetration defects, *Sci. Technol. Weld Join.*, 7(5), 306–312.
22. **Singh P.J., Guha B., Achar D.R.G.** (2003), Fatigue life prediction using two stage model for AISI 304L cruciform joints, with different fillet geometry, failing at toe, *Sci. Technol. Weld. Join.*, 8(1), 69–75.
23. **Sonsino C.M., Fricke W, de Bruyne F., Hoppe A., Ahmadi A., Zhang G.** (2012), Notch stress concepts for the fatigue assessment of welded joints – Background and applications, *Int. Journal of Fatigue*, 34(1), 2–16.
24. **Stenberg T., Barsoum Z., Balawi S.O.M.** (2015), Comparison of local stress based concepts — Effects of low-and high cycle fatigue and weld quality, *Engineering Failure Analysis*, 57, 323–333.
25. **Tchoffo Ngoula D., Beier H. Th., Vormwald M.** (2017), Fatigue crack growth in cruciform welded joints: Influence of residual stresses and of the weld toe geometry, *International Journal of Fatigue*, 101(2), 253–262.
26. **Tsuji I.** (1990), Estimation of stress concentration factor at weld toe of non-load carrying fillet welded joints, *Trans West Jpn Soc Naval Architects*, 80, 241–251.
27. **Ushirokawa O., Nakayama E.** (1983), Stress concentration factor at welded joints, *Ishikawajima–Harima Eng. Rev.*, 23(4), 351–355.
28. **Wooryong P., Chitoshi M.** (2008), Fatigue assessment of large-size welded joints based on the effective notch stress approach, *International Journal of Fatigue*, 30(9), 1556–1568.
29. **Young J.Y., Lawrence F.V.** (1985), Analytical and graphical aids for the fatigue design of weldments, *Fatigue Fracture Eng Mater Struct.*, 8(3), 223–241.
30. **Zerbst U., Madia M., Schork B.** (2016), Fracture mechanics based determination of the fatigue strength of weldments, *Procedia Structural Integrity*, 1, 10–17.